DETERMINATION OF MATERIAL COEFFICIENTS FOR A NON-LINEAR VISCOUS FLUID BY A NUMERICAL INVERSE ANALYSIS AND ITS VERIFICATION WITH A FINITE ELEMENT SIMULATION

B. E. Abali [1] , W. H. Müller [2]

Summary: *Non-linear constitutive relations are used to model some rheological materials, such as melting polymers, semi-solid emulsions, or cosmetic creams. Two different non-*NEWTON*ian fluid models are introduced, and we discuss how to fit the unknown material coefficients from experiments. A rotational viscometer is used for collecting the data and a non-linear least-squared error minimization is utilized to determine the coefficients by an inverse analysis. Both of the models already show promising results in one-dimensional analysis. Moreover, a successful two-dimensional numerical verification was performed, using finite difference and finite element methods, completing an automated experiments-curve fit-validation procedure for engineering science.*

Keywords: *non-linear constitutive relations, inverse analysis, numerical modeling*

1 Introduction and experimental setup

In our daily life, we encounter many highly viscous materials, such as slurry cement, ketchup, toothpaste, etc. Modeling their flow behavior as accurately as possible enables us to predict the material response without further experiments. This is achieved first by selecting a non-linear material and determining the material coefficients for that model with an experiment. We use toothpaste as kind of a "semi-solid" material in a rotary viscometer. Second, the measured response is used to obtain the material coefficients by an inverse analysis. We implement a non-linear optimization scheme for that sense. Third, the strength of the model is validated by simulating the experiment where we applied finite element method.

One of the early treatments for a cone-plate viscometer can be found in [1]. We basically use the same mechanical apparatus, a cone with an angle of $4°$ and a diameter of 60 mm as drawn on the left in Fig. 1, equipped with a Texas Instruments controller unit. By choosing the small cone angle edge effects are reduced. Clearly, viscous fluids will produce heat during the flow. However, using a cone with a small gap to the plate leading to a relatively large surface to volume ratio, will enable a sufficiently quick heat exchange to the environment so that the assumption of an isothermal state is admissible. In our experiments, we used Signal toothpaste, however, for the sake of comparison we could not find any experimentally obtained material coefficients of a material model from the literature. The measurement is performed by controlling the stress, since we expect a Bingham type behavior (cf., Section 2) where the fluid flows after the "yield stress" has been reached.

[1] B. Emek Abali, M.Sc., Institute of Mechanics, Chair of Continuum Mechanics and Materials Theory, Technical University of Berlin, Sekr. Ms2, Einsteinufer 5, 10587 Berlin, Germany, email: abali@tu-berlin.de

[2] Prof. Dr. rer. nat. Wolfgang H. Müller, Institute of Mechanics, Chair of Continuum Mechanics and Materials Theory, Technical University of Berlin, Sekr. Ms2, Einsteinufer 5, 10587 Berlin, Germany,

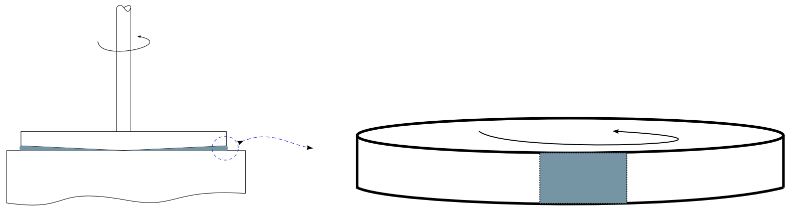

Figure 1: Sketch of the cone-plate apparatus (left) and the extraction of the domain on the outer shell for the numerical simulation (right).

2 Constitutive relations

There are many different material models for highly viscous fluids available. We use the word "fluid" as a term for the material with the behavior under loading such that the motion of its particles does not recover fully after unloading. In a viscometer the matter is driven by applied forces which create stresses and the material model gives the relation between CAUCHY stress tensor σ_{ij} and (symmetric) velocity-gradients d_{ij}:

$$\sigma_{ij} = \mu d_{ij} \; , \; d_{ij} = \frac{\partial v_{(i}}{\partial x_{j)}} = \frac{1}{2}\Big(\frac{\partial v_i}{\partial x_j} + \frac{\partial v_j}{\partial x_i}\Big) \; . \tag{1}$$

Hence by choosing a constant viscosity μ, as being the case in the NAVIER-STOKES model, the interaction between stress and velocity-gradients is linear and they are linked to each other component-wise. Therefore one component of stress, e.g. σ_{12}, depends linearly on the corresponding velocity-gradient, thus on d_{12}. However, there are materials which respond differently to different magnitudes of velocity-gradients, known as non-NEWTONian fluids. In order to describe such phenomena, many different techniques are used. One of the earliest attempts by Herschel and Bulkley [2] was to change the constant μ to an *apparent* viscosity depending on the *shear rate* which is the one component of the velocity-gradients, d_{12}. Quite often the three-parameters HERSCHEL-BULKLEY model, given by a power law, is used:

$$\sigma_{12} = \mu (d_{12})^n + \tau \; . \tag{2}$$

It is motivated by experimental results, thus presented in the latter, one-dimensional form. We propose to transfer that idea to multiaxial tensor notation as follows:

$$\sigma_{ij} = \Big(\mu \frac{(II_d)^{n/2}}{\sqrt{II_d}} + \frac{\tau}{\sqrt{II_d}}\Big) d_{ij} \; , \; II_d = \frac{1}{2} d_{ij} d_{ij} \; , \tag{3}$$

since in case of a shear deformation, i.e., $d_{ij} = \begin{pmatrix} 0 & d_{12} \\ d_{12} & 0 \end{pmatrix}$, $II_d = (d_{12})^2$, the Eq. (3) reduces to the Eq.(2) such that: $\begin{pmatrix} 0 & \sigma_{12} \\ \sigma_{12} & 0 \end{pmatrix} = \mu \frac{(d_{12})^n}{d_{12}} \begin{pmatrix} 0 & d_{12} \\ d_{12} & 0 \end{pmatrix} + \frac{\tau}{d_{12}} \begin{pmatrix} 0 & d_{12} \\ d_{12} & 0 \end{pmatrix}$.

By using a completely different, more theoretical motivation Ziegler [3, 4] proposed the following non-linear constitutive relation for non-linear viscous materials:

$$\sigma_{ij} = \mu' d_{ij} + \frac{2\tau'}{\pi \sqrt{II_d}} \arctan\Big(\frac{\sqrt{II_d}}{n'}\Big) d_{ij} \; . \tag{4}$$

Its reduction to one-dimensional space for the parameter fit reads:

$$\sigma_{12} = \mu' d_{12} + \frac{2\tau'}{\pi} \arctan\Big(\frac{|d_{12}|}{n'}\Big) \operatorname{sign}(d_{12}) = \mu' d_{12} + \frac{2\tau'}{\pi} \arctan\Big(\frac{d_{12}}{n'}\Big) \; . \tag{5}$$

Though it is not immediately obvious, both relations will turn into the BINGHAM material model as used in Bingham [5] and Houwink [6] through the limiting case: $n = 1 \; , \; n' = \infty \Rightarrow \mu = \mu \; , \; \tau = \tau' \; , \; \sigma_{ij} = \mu d_{ij} + \frac{\tau}{\sqrt{II_d}} d_{ij}$. In this representation the yield shear stress, τ, and the viscosity, μ, are physically meaningful rheology constants.

3 Parameter fit

Instead of calculating the response of the material by known parameters, we measure the shear-rate as the output variable and by using this data obtain the corresponding model parameters inversely. It is possible to find the three parameters μ, n, τ in the first model (Eq. 2) or μ', n', τ' in the second model (Eq. 5) by measuring three different stress, velocity-gradient states, i.e., $\{\sigma_{12}, d_{12}\}$, and then by solving the inverse problem directly. However, it is an experimental fact that we get much more than just three states. Then the inverse problem has many solutions, each of every one fits at least to three different states. In this case the optimum solution can be determined in terms of an error prediction, i.e., *cost*, which is minimized numerically to obtain the best parameters. We programmed and solved the inverse problem in SciPy [7] by using the Levenberg-Marquardt non-linear least squares error algorithm for measurements analyzed by Eqs. 2 and 5. Unfortunately the optimization is non-linear and thus depends on the starting parameter. Therefore in a parameter-range we randomly select starting parameters and compare the cost. This is known as *Monte Carlo* method since the starting parameters are chosen randomly. The best solution is never guaranteed but the possibility of getting the optimum solution increases upon every new trial. At the end of the optimization the following results are obtained:

$$\mu = 220.056 \text{ Pa s}\,,\ n = 0.599\,,\ \tau = 5.420 \text{ Pa}\,,\ \mu' = 61.446 \text{ Pa s}\,,\ n' = 0.267\,,\ \tau' = 190.217 \text{ Pa}\,. \tag{6}$$

4 Numerical modeling

The balance law for mass $\frac{\mathrm{d}\rho}{\mathrm{d}t} + \rho\frac{\partial v_i}{\partial x_i} = 0$ and for linear momentum $\rho\frac{\mathrm{d}v_i}{\mathrm{d}t} - \frac{\partial \sigma_{ji}}{\partial x_j} = \rho f_i$ have to be satisfied. After neglecting the volume forces f_i, their arbitrary variations in a HILBERT configuration space form an invariant:

$$\int_\Omega \Big(\frac{\mathrm{d}\rho}{\mathrm{d}t} + \rho\frac{\partial v_i}{\partial x_i}\Big)\delta\rho + \Big(\Big(\rho\frac{\mathrm{d}v_i}{\mathrm{d}t} - \frac{\partial \sigma_{ji}}{\partial x_j}\Big)\delta v_i\Big)\,\mathrm{d}v = 0\,, \tag{7}$$

which can be minimized in a discrete manner. We discretize in time with a finite difference method:

$$\frac{\mathrm{d}}{\mathrm{d}t}\Big(\cdot\Big) = \frac{\partial}{\partial t}\Big(\cdot\Big) + \frac{\mathrm{d}x_i}{\mathrm{d}t}\frac{\partial}{\partial x_i}\Big(\cdot\Big) = \frac{(\cdot)-(\cdot)^0}{t-t^0} + v_i\frac{\partial}{\partial x_i}\Big(\cdot\Big)\,,\ \mathrm{d}t = t - t^0\,,\ v_i = \frac{\mathrm{d}x_i}{\mathrm{d}t}\,, \tag{8}$$

and in space with a finite element method:

$$\int_{\Omega^{\text{ele.}}} \Big(\frac{\rho-\rho^0}{t-t^0}\delta\rho + v_i\frac{\partial \rho}{\partial x_i}\delta\rho + \rho\frac{\partial v_i}{\partial x_i}\delta\rho + \rho\frac{v_i - v_i^0}{t-t^0}\delta v_i + \rho v_j\frac{\partial v_i}{\partial x_j}\delta v_i + \sigma_{ji}\frac{\partial \delta v_i}{\partial x_j}\Big)\,\mathrm{d}v - \oint_{\partial\Omega} \sigma_{ji}\delta v_i n_j\,\mathrm{d}a\,, \tag{9}$$

where integration by parts has been used to get only first-order differentials in velocities v_i, which can be approximated with linear (in space) elements. This form is non-linear in velocities, hence first it is linearized on the partial differential level with the NEWTON-RAPHSON method and solved incrementally in each time step within the FEniCS project [8]. All the boundaries except the top are set to traction-free, so that the last term vanishes and the rectangular cavity with periodic boundaries on right and left is driven on top with a linearly raising traction and hold on bottom. This creates the outer shell of the cone-plate, as seen in Fig. 1, where also the measurement data is taken.

5 Concluding remarks

Two different constitutive relations are used to model the toothpaste, which shows non-linear behavior under linearly arising moment, thus stress. Both of the models can fit the measurement data nicely and the parameters in Eq. 6 seem physically admissible and consistent with each other. Subsequently a simulation by utilizing the fit parameters is implemented to extract the same data as been measured. The perfectly accurate results from both models with the experiments and numerical solution in Fig. 2 show the strength of the procedure. The second model can capture the curvature much better, especially in the region of higher stresses, thus it seems to be more useful for fluid flow simulations. For the sake of encouraging further research, we supply all the data and the code in [9] under GNU Public license [10].

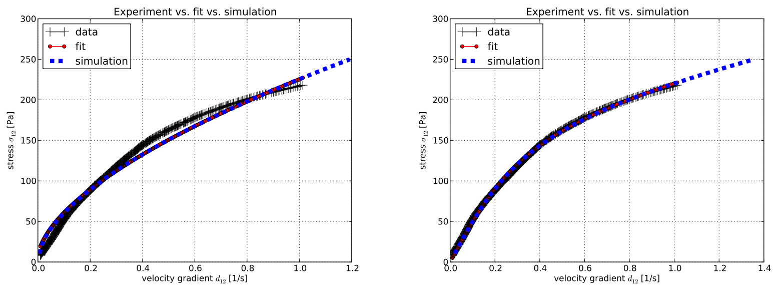

Figure 2: Left for the first and right for the second model, data from the experiment in black, fit curve in 1D in red, simulation in 2D in blue.

References

[1] McKennell R. *Cone-plate viscometer, comparison with coaxial cylinder viscometer*, Anal. Chem. 28(11), 1710–1714 (1956).

[2] Herschel, W. H., Bulkley, R. *Konsistenzmessungen von Gummi-Benzollösungen*. Kolloid-Z. 39, 291–300 (1926).

[3] Ziegler, H. *An introduction to thermomechanics*. North Holland, Amsterdam, 1977.

[4] Ziegler, H., Wehrli, C. *The derivation of constitutive relations from the free energy and the dissipation function*. Advances in Applied Mechanics 25, 183 – 238 (1987).

[5] Bingham, E. C. *Fluidity and plasticity*, McGraw-Hill Book Company, Inc., New York, 440, 1922.

[6] Houwink, R. *Elasticity, plasticity and structure of matter*. Cambridge University Press,1937.

[7] Eric, J., Travis, O., Pearu, P., et al. *SciPy: Open source scientific tools for Python*, 2001–.

[8] Logg, A., Mardal, K. A., Wells, G. *Automated solution of differential equations by the finite element method: The FEniCS book*. Springer, 2012.

[9] Abali, B. E., *Technical University of Berlin, Institute of Mechanics, Chair of Continuums Mechanics and Material Theory, Computational Reality*. http://www.lkm.tu-berlin.de/ComputationalReality/, 2011–.

[10] Gnu Public *Gnu general public license*. http://www.gnu.org/copyleft/gpl.html.